Romanian Reports in Physics **69**, 411 (2017)

OPERATING THE HIPIMS DISCHARGE WITH ULTRA-SHORT PULSES: A SOLUTION TO OVERCOME THE DEPOSITION RATE LIMITATION

I.-L. VELICU[1], I. MIHAILA[2], G. POPA[1]

[1] "Alexandru Ioan Cuza" University, Faculty of Physics, Iasi – 700506, Romania,
E-mails: laura.velicu@uaic.ro; ghpopa@uaic.ro
[2] Integrated Center of Environmental Science Studies in the North-Eastern Development Region (CERNESIM), Alexandru Ioan Cuza University of Iasi, Iasi – 700506, Romania,
E-mail: ilarion.mihaila@gmail.com

Received July 30, 2016

Abstract. This study presents results on the influence of pulse duration in HiPIMS discharge on the sputtering mechanisms, target-to-substrate particles transport, and deposition rate. A copper disk-shaped target was sputtered in argon atmosphere, increasing the pulse duration from 3 μs to 50 μs and adjusting the pulsing frequency in order to keep a constant average power of 100 W. Voltage and current waveforms, time-resolved fast imaging, time resolved-optical emission spectroscopy, time evolution of the ion flux towards the substrate, and energy-resolved mass spectrometry were used in order to investigate the plasma composition and its change in front of the target. Increasing the pulse duration, the sputtering mechanism is gradually transformed from dominant gas sputtering to self-sputtering driven mode and the deposition rate decreases.

Key words: HiPIMS, self-sputtering, sputtering wind, deposition rate, plasma diagnostics.

1. INTRODUCTION

The physical vapour deposition (PVD) techniques based on magnetron sputtering are already widespread in the global manufacturing of thin films and coatings. The requirements of the emerging technology for satisfying the need of high-quality materials with specific applications led to numerous attempts to improve and develop the conventional PVD techniques.

In the field of ionized PVD techniques, high power impulse magnetron sputtering (HiPIMS) is a relatively new deposition technique which has been shown to produce thin films with improved properties, in particular in terms surface roughness, density and adhesion to a substrate. In HiPIMS, very high instantaneous power is applied to the target with a low duty factor and low frequencies, maintaining the time-averaged target power density in values

comparable to those used in the conventional *dc* magnetron sputtering (dcMS) [1]. The target power densities can reach levels of several kW/cm^2, producing energetic deposition ions with energies in the range of tens of eV. Moreover, due to ultra-high density plasma, the deposition flux is largely ionized, increasing both its reactivity in the gas phase and the deposited energy at the substrate [2, 3]. The high ion-to-neutral ratio and energetic ion flux towards the substrates have been shown to enable the deposition of ultra-dense and smooth metallic and compound films with higher adhesion to the deposition substrate. Regarded as a source for ionization of sputtered material, HiPIMS offers the possibility of growing high-quality thin films by sputtering a wide range of elemental and composite materials [4] and allows deposition on complex shaped substrates [5]. These advantages together with the excellent control on the energy and direction of the deposition flux opened up new perspectives and horizons in the area of coatings deposition.

Even if HiPIMS is industrially and commercially viable, very little is known on the details of the process parameters existing in a typical HiPIMS system and its understanding is still under research and development. In spite of its great perspective, this deposition technique, especially in non-reactive regime, has a major drawback: the reduction of the power normalized deposition rate as compared to the rates achieved in dcMS discharge operated in the same working conditions. It was found that, depending on target material, the deposition rates are typically in the range of 20–80% compared to dcMS [6, 7].

The main causes considered to be responsible for this loss deposition rate are known, but overall not fully understood. Therefore, the most important factors that may lead to relatively low deposition rates in HiPIMS are:

(*i*) *ion return effect* – the back-attraction of sputtered material (ionized close to the target) followed by self-sputtering causes a reduction in the amount of sputtered particles reaching the substrate since the sputtering yield of a target material when is bombarded by ions from the same element is typically lower than the Ar-sputtering yield [8, 9];

(*ii*) *transport effect* – strong axial potential gradients in the HiPIMS plasma that prevent the transport of low energy post-ionized metal ions to the substrate [10] and their side-wall loss due to the radial transport [11]. Lundin *et al.* showed that a significant fraction of ions is transported radially away from the cathode, while only a small fraction of ions may be available for deposition of a substrate facing the target, reducing in this way the deposition rate [12];

(*iii*) *gas rarefaction effect* – significant gas rarefaction that can occur for longer HiPIMS pulses (>50 μs), causing a decrease in the Ar ion density available for sputtering [13]. The gas rarefaction effect is assumed to occur mainly through heating and corresponding thermal expansion, where heating is due to the collisions between the background gas and the sputtered target atoms, as well as reflected sputtering gas atoms;

(*iv*) *sputtering yield effect* – caused by the less than linear increase of the sputtering yield with increasing ion energy [14]. HiPIMS operates at high cathode voltage and, as a consequence, the instantaneous power increasing does not lead to a corresponding linear increase in sputtering yield.

The lower HiPIMS deposition rate as compared to the rates achieved in dcMS discharge, operated at the same average power, was attributed to the higher energies per pulse dissipated in the plasma accompanied by a change in the plasma chemistry. The amount of sputtered material during the pulse did, in fact, significantly increase, but self-scattering prevented a more efficient transport. From an economic point of view, this might be a big disadvantage of HiPIMS and it may overshadow its great advantages in manufacturing coatings with enhanced properties. This is the reason why increasing the deposition rate in HiPIMS is still a challenging task in the industrial and academic research community.

During the ignition phase of HiPIMS discharge, the plasma potential is strongly negative and its spatial structure in the magnetic trap region provides a large potential barrier for the sputtered ionized species, avoiding their transport to the substrate. The sputtered ionized species are back-attracted to the target by the large axial electric field and strongly accelerated in the cathode fall, causing self-sputtering effect and diminishing the deposition rate [15]. Numerous attempts have been proposed to improve the deposition rates in HiPIMS by using an appropriate magnetic field configuration and/or pulsing design. Capek *et al.* have shown that lowering the magnetic field in HiPIMS can have a significant effect on increasing the deposition rate [16]. Similar results have been found by Mishra *et al*. who showed that deforming the magnetron's magnetic field changes the plasma sheath properties and improves the ion transport towards the substrate [10]. Decreasing the magnetic field strength, the sheath region in front of the target becomes wider and plasma potential distribution inside the magnetic trap is changed. The electrical field across the cathode sheath becomes lower and a large fraction of ionized sputtered particles can escape from the magnetic trap [17].

It has been also observed that the HiPIMS operated in short pulse mode allows both increasing the deposition rate due to the reduced gas rarefaction effect and reducing the ion back-attraction effect of the ionized sputtered material [18, 19]. Antonin *et al.* [20] showed that exciting the HiPIMS plasma in multi-pulse mode by applying sequences of five micro-pulses (3 μs in length) separated by 50 μs can increase the deposition rates by up to 50%. In HiPIMS discharge, the peak target current is a key factor in controlling the power normalized deposition rate. Tiron *et al.* demonstrated that the deposition rate can be manipulated through the peak target current (pulse energies), which in turn can be controlled by certain discharge operation parameters such as: target voltage, pulse duration, magnetic field configuration, target erosion depth, and operation mode [21]. It is thus suggested that short pulses and high frequencies should be used in order to improve the deposition rate in HiPIMS.

The aim of this paper is to understand the deposition rate limitation in the HiPIMS discharge and to present a solution able to overcome this drawback. Cathode voltage and current waveforms, fast imaging, time-resolved optical emission spectroscopy, deposition rate and time-averaged ion current measurements, and energy-resolved mass spectrometry were used for this purpose.

2. EXPERIMENTAL DETAILS

Figure 1 presents the schematic diagram of the HiPIMS system together with some of the plasma diagnostics devices used in this work, which will be described in detail hereinafter. High power pulses were applied to a balanced planar circular magnetron equipped with a copper target (50 mm diameter and 3 mm thickness). High power pulses were provided to the target by a pulse generator charged by a *dc* power supply (Heinzinger PNC 3500–500 ump). The pulse voltage was set by the *dc* charging unit to –1 kV and monitored by a 1:100 voltage probe (Tektronix), connected to the target feedthrough, while the pulse duration and repetition rate were handled by the pulse unit. The current was measured using a broadband inductive current monitor (0.1V/A*)*. All the electrical signals were recorded and stored on a digital oscilloscope (LeCroy Wave Surfer 434). The high power pulse system allows superposition of a pre-ionization low current (4 mA) *dc* discharge with high voltage pulses applied directly on the magnetron cathode. The pre-ionization low current discharge creates low density plasma near the magnetron cathode, which provides a plasma sheath already established before applying the high voltage pulse. The presence of the initial plasma sheath ensures the fast and reproductive cathode current dynamics when high voltage is applied.

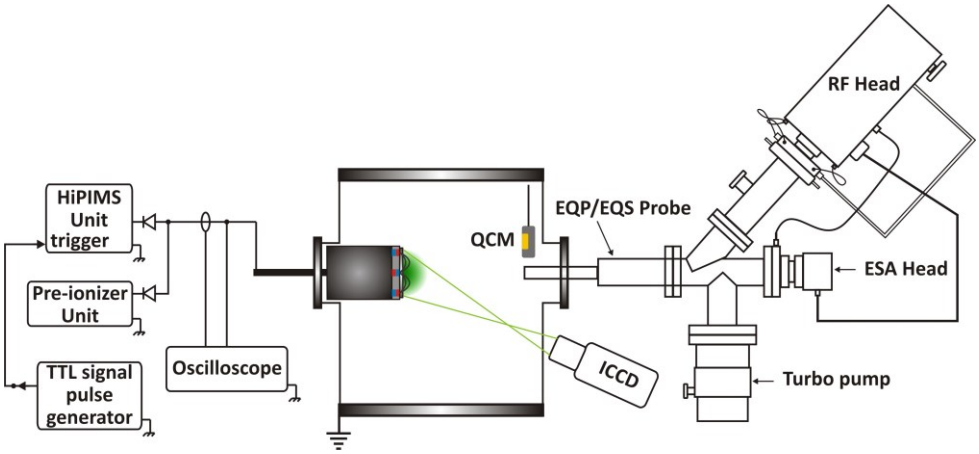

Fig. 1 – Schematic view of the experimental setup including the HiPIMS system, quartz crystal microbalance (QCM), ICCD camera (ICCD), and mass spectrometer.

The magnetron was housed in a vacuum chamber (40 cm in height and 40 cm in diameter), which was pumped down to a base pressure of 1×10^{-5} Pa by a turbo-molecular pump backed by a dry scroll pump. The target was sputtered at different pulsing frequencies, with pulse duration ranged from 3 μs to 50 μs, in argon gas environment, using a working gas pressure of 1 Pa. For each value of the pulse length, the pulsing frequency was varied until the average power of 100 W was achieved.

The Time Resolved-Optical Emission Spectroscopy (TR-OES) was used for finding and comparing temporal evolutions of argon and copper excited atoms during the pulse discharge. The high density plasma region in front of the cathode was monitored through a quartz window mounted in lateral side of the target, using an optical fiber which guides the light to a monochromator having a photomultiplier as detector.

Information on the ion flux at the substrate region was obtained using a cold electrostatic probe (disc shape of 1.5 cm diameter), axially placed at a distance of 10 cm from the cathode discharge. The probe was negatively biased (–100 V) with respect to the anode, using a *dc* power supply. The time evolution of the probe current intensity during the pulse discharge was stored on the oscilloscope.

The time-resolved fast imaging technique was also used for finding, at certain instant time, the spatial distribution of both gas atom (Ar) and sputtered material (Cu) excited species. The side-view images of the HiPIMS discharge were registered with s fast ICCD camera (Hamamatsu), using an exposure gate of 30 ns. The time evolutions of argon and copper excited species were separately registered using optic selective filters: a red filter with transmission band in the range of 695–1100 nm for Ar spectral lines and a green filter with transmission band in the range of 485–550 nm for Cu.

The plasma composition, time averaged Cu ion energy distribution and integral flux were recorded with an energy-resolved mass spectrometer (HPR60 Hiden Analytical [22]) placed in a position directly facing the target surface at a distance of 10 cm. The integral flux of Cu ions was determined by a direct integration of the time-averaged ion energy distribution.

The deposition rate was monitored using a Quartz Crystal Microbalance (Inficon Q-pod, equipped with 6 MHz quartz crystal oscillator and gold coated sensor), placed axially at a distance of 100 mm from the target's surface. The deposition rate was estimated from the total thickness of the deposited film, measured over a fixed deposition time of 100 s.

3. RESULTS AND DISCUSSION

3.1. CURRENT AND VOLTAGE WAVEFORMS

Figure 2 presents the time evolution of magnetron voltage and discharge current intensity for pulse durations of 3 μs (Fig. 2a) and 50 μs (Fig. 2b), respectively. The HiPIMS current pulse develops through several steps. Thus, when voltage is applied, the plasma density in the chamber is negligible and the discharge has to be ignited. An electron wave, characterized by high electrons energy, propagates through the chamber and initiates the discharge ignition. As the discharge current starts to rise, it reaches values of tens of amperes in few micro-seconds and the discharge dissipates a very high instantaneous power. There is a slight delay between the discharge current and cathode voltage onset because the discharge breakdown through the ionizing collision cascade needs some time to propagate. In the first case, the absolute discharge voltage value presents a slight decrease during the pulse, while the pre-ionization voltage is approximately zero. When the HiPIMS discharge is operated with long pulses, the absolute pre-ionization voltage value increases up to 320 V and the absolute discharge voltage exhibits an abrupt decrease to approximately 500 V within the first 15 μs.

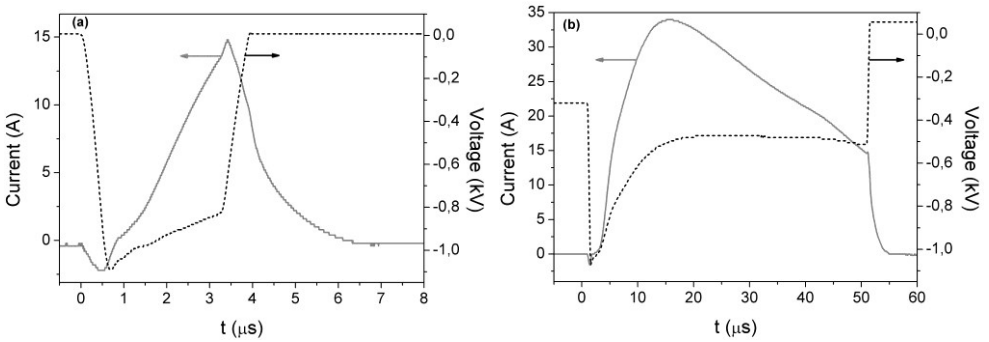

Fig. 2 – Discharge current intensity and voltage waveforms for:
a) short pulses of 3 μs; b) long pulses of 50 μs.

The discharge current evolution is even more different for the two selected cases. For short pulses, it reaches a maximum value of about 15 A in about 2.5 μs and then drops quickly to zero. In the second case, the discharge current intensity increases up to approximately 35 A within the first 15 μs and then decreases, due to gas rarefaction, before settling on a steady-state value. Regardless the pulse duration, during the initial phase (1–4 μs after the voltage is applied), the temporal evolution of the discharge current intensity is approximately the same, meaning

that in this phase, plasma will always have the same composition, being composed mainly of gas species. Increasing the pulse duration, the electron density will also increase producing high density plasma in the cathode vicinity, with species largely dominated by the Cu ions and excited atoms. Therefore, increasing the pulse duration, the sputtering mechanism is gradually transformed from dominant gas sputtering to self-sputtering driven mode.

3.2. FAST IMAGING (ICCD)

Fast imaging technique, consisting of ICCD camera in conjunction with bandpass optical filters, enable time-resolved investigation of physical and chemical properties of transient plasma discharges. In this study, the dynamics of the HiPIMS plasma and its composition evolution with increasing the pulse duration, as well as the onset of the self-sputtering regime were investigated using lateral images of the plasma, recorded using an ICCD camera. The ICCD camera was synchronized with the voltage pulse driving the magnetron plasma discharge. Figure 3 presents on-pulse lateral ICCD images registered with red (left, argon) and green (right, copper) bandpass optical filters at 3 μs and 50 μs, respectively.

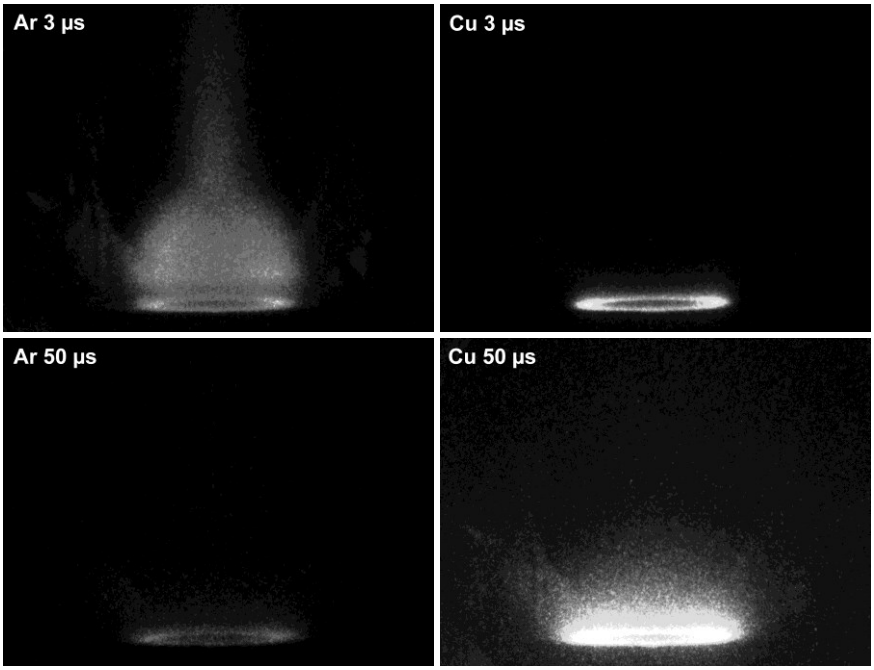

Fig. 3 – On-pulse fast ICCD images registered at 3 μs and 50 μs respectively, with red (Ar) and green (Cu) bandpass optical filters.

The optical filters allow to distinguish different phases of the discharge and to investigate the dynamics of gas and metallic species [23]. These images clearly show that in the HiPIMS plasma, in the first 3 μs after the voltage is applied, the optical radiation comes mainly from the excited atoms of the working gas. At the end of the pulse, 50 μs after the voltage is applied, the excited argon atoms emission becomes very weak and the optical radiation is dominated by the emission from the excited Cu atoms.

3.3. TIME-RESOLVED OPTICAL EMISSION SPECTROSCOPY (TR-OES)

Time-resolved optical emission spectroscopy can be used for monitoring the time variation of the plasma composition during the pulse. Figure 4 shows the time evolution of atomic spectral line intensities emitted by Ar I (750.4 nm) and Cu I (521.8 nm) during voltage pulses with amplitude of –1 kV and duration of 3 and 50 μs, respectively. These measurements have been performed in the cathode surface vicinity, for pulse duration of 3 and 50 μs.

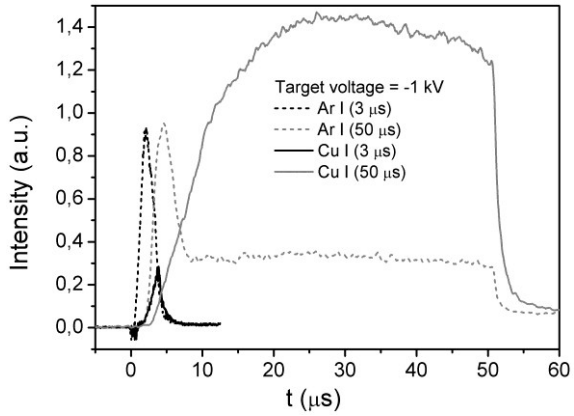

Fig. 4 – Time evolution of Ar I and Cu I atomic spectral line intensities during on pulse of 3 and 50 μs, respectively.

As it can be seen, the intensity of atomic spectral line corresponding to the excited argon neutrals increases almost simultaneously with the voltage pulse applied on the target and its time evolution coincides with the target voltage waveform. The fast onset of Ar emission can be explained based on the fact that the buffer gas atoms are permanently present in the discharge space and, during the initial phase of the pulse, they are collided by the highly energetic electrons. Regardless the pulse duration, the Ar emission line has approximately the same amplitude and shape, the only difference being that the peak corresponding to long voltage pulse durations (50 μs) is shifted to the right due to the delay of the

discharge ignition. According to voltage waveforms presented in Fig. 2(b), for long pulses of 50 μs, the absolute pre-ionization voltage is approximately 320 V. This means that for long pulses, in the pre-ionization phase, there is a very weak plasma in the discharge volume and the discharge breakdown through the ionizing collision cascade needs more time to propagate. After approximately 5 μs, due to the onset of the sputtering flux emerging from the target (sputter wind), a local gas rarefaction in front of the target will appear and the argon line intensity will start to decrease. At this time, the Ar content diminishes quickly due to the intense production of metal ions and rarefaction of the gas by the high power dissipated in the pulse. The intensity of Cu atomic spectral line starts to increase only after the target current intensity reaches high values and the sputtered atom density in front of the target has increased significantly. The Cu spectral line has the same evolution as the discharge current because the Cu atoms are sputtered from the target by ion bombardment and the discharge current measured at the cathode is carried out by the ions. Its evolution reaches its maximum after 20 μs and then slightly decreases. There is a huge difference in amplitude between the Cu spectral lines emitted at short (3 μs) and long (50 μs) pulse durations, indicating once again the presence of two distinct sputtering modes. In other words, the first phase of the pulsed discharge, when target voltage is very high and current is low, the plasma composition is dominated by the working gas species (gas sputtering mode), while the second one, when target voltage is low and current is high, is strongly influenced by the metallic species (self-sputtering regime). As the pulse duration is increased, more copper ions will be in the dense plasma region near the cathode and some of them will be accelerated back to the target, initiating the self-sputtering regime.

3.4. DEPOSITION RATE AND TIME-AVERAGED ION CURRENT MEASUREMENTS

The deposition rate, time-average probe current and Cu ions flux *versus* pulse duration are presented in Fig. 5. The pulse duration was varied between 3 and 50 μs, while the repetition frequency was ranged between 5 kHz and 150 Hz in order to keep the same time-average power delivered to the HiPIMS discharge. Increasing the pulse duration from 3 to 50 μs, the pulse energy also increases, almost linearly, from 20 mJ to 600 mJ. The influence of pulse duration on the deposition rare was investigated and the obtained results are explain based on the total ion current and Cu ion flux measured at substrate position using an electrostatic probe and a mass spectrometer, respectively. The deposition rate *versus* pulse duration is very well correlated with the total ion current and Cu ion flux, all physical parameters exhibiting the same behaviour (fast decrease) as the pulse duration increases from 3 to 10 μs. Increasing the pulse duration beyond 10 μs, the total ion current and Cu ion flux slightly decrease, while the deposition

rate continues to decrease as the pulse duration is enlarged up to 20 μs and then slightly increases.

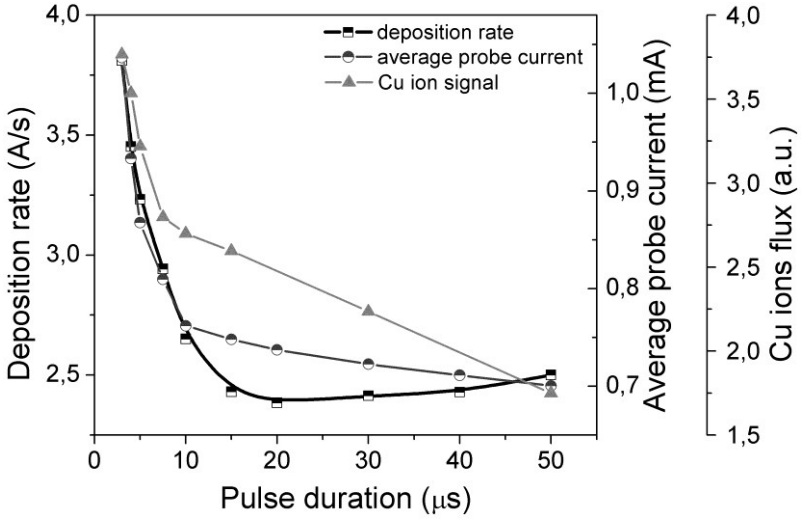

Fig. 5 – Deposition rate, average probe current and Cu ions flux dependence on the pulse duration.

Keeping in mind that the loss of sputtered material may be attributed to the back-attraction of ions created close to the target surface, the most straightforward interpretation for the decrease of total ion current and Cu ion flux is that the fraction of back-attracted ions increases with pulse energy. This ion fraction returning to the target contributes to the discharge current, a very important parameter included in the power normalized deposition rate. The slight increase of the deposition rate, for pulse durations longer than 20 μs, may be attributed to the gradually change of sputtering regime from HiPIMS to dcMS due to the reduced instantaneous power within the long pulse *via* discharge current.

3.5. ION ENERGY DISTRIBUTION FUNCTION (IEDF)

More valuable information can be extracted from the ion energy distribution functions of Cu ions recorded by energy-resolved mass spectrometry. Figure 6 presents time-averaged energy distributions of Cu^{1+} ions for two selected pulse durations. Both distributions contain a low energy peak centered at about 1.5 eV (short pulses of 3 μs) and 2.5 eV (long pulses of 50 μs), respectively. This low energy peak, broader when the HiPIMS discharge is operated with short pulses, can be regarded as being related to low energy and thermalized copper ions as result of the scattering process on the buffer gas atoms during the transport towards the

mass spectrometer head. Beside the low energy peak, both distributions contain a shoulder (much more visible for long pulses) and a high-energy tail extending up to 100 eV. The high-energy tail structure is related to the original energy distribution of the sputtered neutrals (Thomson distribution), which are ionized on their way to the mass spectrometer head. These highly energetic ions include also the ionized species that are reflected by the highly negative target potential as fast neutrals and then ionized by the electron collisions as they pass through the high density plasma [24].

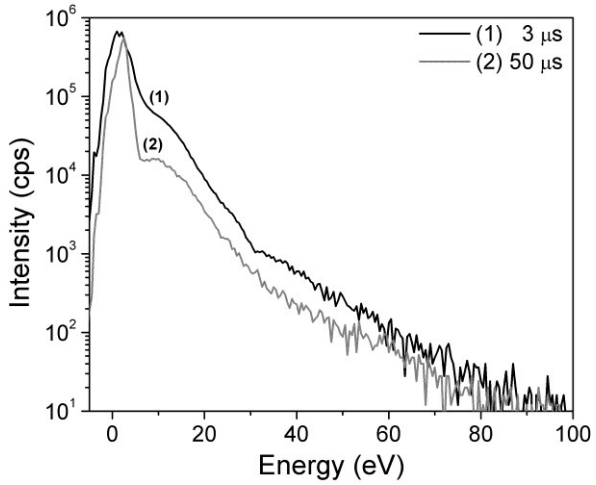

Fig. 6 – Time averaged ion energy distribution of Cu^{1+} for selected pulse durations.

Although the amount of Cu ions produced during a long pulse (50 μs) is higher than the one produced during a short pulse (3 μs), when the HiPIMS discharge operates with same average power (100 W), the total amount of Cu ions reaching the substrate, in certain period of time, is higher for short pulse operation mode. This can be explained by taking into account that, for the same average power, the repetition frequency of the short pulses (5 kHz) is much higher than that used for long pulses (150 Hz).

Experimental results showed that the deposition rate increases significantly when the HiPIMS discharge is excited with very short voltage pulses at high repetition frequency because this operation mode does not allow a significant amount of gas rarefaction or self-sputtering to develop at the target, favoring the production of ions in plasma volume, away from target, and preventing their back-attraction. Moreover, the high pulsing frequency leads to a significant improvement in plasma conductivity and to a better ions transport towards substrate.

4. CONCLUSIONS

In HiPIMS, the deposition rate can be controlled, among other discharge operation parameters, through the pulse voltage duration. In order to study the influence of pulse duration on the deposition rate, sputtering mechanisms, and target-to-substrate particles transport, a copper target was sputtered under argon atmosphere. The pulse duration was increased from 3 to 50 μs and the pulsing frequency was adjusted in order to keep a constant average power of 100 W.

According to the cathode voltage and current waveforms and fast imaging results, during the initial phase of the pulse, the HiPIMS plasma is composed mainly of gas species. Increasing the pulse duration, the high density plasma in the cathode vicinity consists mainly of Cu ions and excited atoms.

The time-resolved optical emission spectroscopy results showed that the intensity of the atomic spectral line corresponding to Ar I increases almost simultaneously with the voltage pulse applied on the target. After approximately 5 μs, due to the sputtering wind, a local gas rarefaction in front of the target appears and the argon line intensity starts to decrease.

The energy-resolved mass spectrometry results of the deposition flux (Cu^{1+} ions) highlighted the existence of two distinctive groups: one consisting of low energy and thermalized copper ions and another one consisting of highly energetic ions.

All the obtained results demonstrated that the significant gas rarefaction and self-sputtering that can occur for longer HiPIMS pulses are main physical reasons for the loss deposition rate.

Acknowledgments. This work was supported by "Alexandru Ioan Cuza" University within "UAIC Grants for Young Researchers" competition (project code GI-2015-07). The POSCCE-O 2.2.1, SMIS-CSNR 13984-901, No. 257/28.09.2010 Project, CERNESIM, is also gratefully acknowledged for the mass spectrometry measurements.

REFERENCES

1. J.T. Gudmundsson, N. Brenning, D. Lundin, and U. Helmersson, J. Vac. Sci. Technol. A **30**, 030801 (2012).
2. G. Greczynski and L. Hultman, Vacuum **84**, 1159 (2010).
3. V. Tiron, I.-L. Velicu, M. Dobromir, A. Demeter, F. Samoila, C. Ursu, and L. Sirghi, Thin Solid Films **603**, 255 (2016).
4. M. Osiac, V. Tiron, G.-E. Iacobescu, and G. Popa, Digest Journal of Nanomaterials and Biostructures **9**, 451 (2014).
5. J. Alami, J. T. Gudmundsson, J. Bohlmark, J. Birch, and U. Helmersson, Plasma Sources Sci. Technol. **14**, 525 (2005).
6. M. Samuelsson, D. Lundin, J. Jensen, M. A. Raadu, J. T. Gudmundsson, and U. Helmersson, Surf. Coat. Technol. **202**, 591 (2010).
7. U. Helmersson, M. Lattemann, J. Bohlmark, A. P. Ehiasarian, and J. T. Gudmundsson, Thin Solid Films **513**, 1 (2006).

8. D.J. Christie, J. Vac. Sci. Technol. A **23**, 330 (2005).
9. A. Anders, J. Andersson, and A. Ehiasarian, J. Appl. Phys. **102**, 113303 (2007).
10. A. Mishra, P.J. Kelly, and J.W. Bradley, Plasma Sources Sci. Technol. **19**, 045014 (2010).
11. P. Poolcharuansin, B. Liebig, and J.W. Bradley, Plasma Sources Sci. Technol. **21**, 015001 (2012).
12. D. Lundin, P. Larsson, E. Wallin, M. Lattemann, N. Brenning, and U. Helmersson, Plasma Sources Sci. Technol. **17**, 035021 (2008).
13. D. Horwat and A. Anders, J. Phys. D: Appl. Phys. **41**, 135210 (2008).
14. J. Emmerlich, S. Mráz, R. Snyders, K. Jiang, and J.M. Schneider, Vacuum **82**, 867 (2008).
15. I.-L. Velicu and V. Tiron, Digest Journal of Nanomaterials and Biostructures **9**, 1513 (2014).
16. J. Capek, M. Hala, O. Zabeida, J.E. Klemberg-Sapieha, and L. Martinu, J Phys. D: Appl. Phys. **46**, 205205 (2013).
17. V. Tiron, I.-L.Velicu, F. Ghiorghiu, and G. Popa, Romanian Reports in Physics **67**, 1004 (2015).
18. S. Konstantinidis, J. P. Dauchot, M. Ganciu, and M. Hecq, J. Appl. Phys. **99**, 013307 (2006).
19. I.-L. Velicu, V. Tiron, and G. Popa, Surf. Coat. Technol. **250**, 57 (2014).
20. O. Antonin, V. Tiron, C. Costin, G. Popa, and T.M. Minea, J. Phys. D: Appl. Phys. **48**, 015202 (2015).
21. V. Tiron, I.-L. Velicu, O. Vasilovici, and G. Popa, J. Phys. D: Appl. Phys. **48**, 495204 (2015).
22. S. Dobrea, I. Mihaila, V. Tiron, and G. Popa, Romanian Reports in Physics **66**, 1147 (2014).
23. C. Costin, V. Tiron, J. Faustin, and G. Popa, IEEE Trans on Plasma Sci. **39**, 2482 (2011).
24. A. Ehiasarian, Y. Gonzalvo, and T. Whitmore, Plasma Process. Polym. **4**, S309 (2007).